Edge States and the Quantized Hall Effect in Graphene

Luis Brey[1] and H. A. Fertig[2]
1. Instituto de Ciencia de Materiales de Madrid (CSIC), Cantoblanco, 28049 Madrid, Spain
2. Department of Physics, Indiana University, Bloomington, IN 47405

(Dated: February 6, 2008)

We study edges states of graphene ribbons in the quantized Hall regime, and show that they can be described within a continuum model (the Dirac equation) when appropriate boundary conditions are adopted. The two simplest terminations, zigzag and armchair edges, are studied in detail. For zigzag edges, we find that the lowest Landau level states terminate in two types of edge states, dispersionless and current-carrying surface states. The latter involve components on different sublattices that may be separated by distances far greater than the magnetic length. For armchair edges, the boundary conditions are met by admixing states from different valleys, and we show that this leads to a single set of edges states for the lowest Landau level and two sets for all higher Landau levels. In both cases, the resulting Hall conductance step for the lowest Landau level is half that between higher Landau levels, as observed in experiment.

PACS numbers: 73.43-f,73.20-r,73.23-b

I. INTRODUCTION

Recent progress in the processing of graphite have made possible the isolation of two dimensional carbon sheets, known as graphene[1]. This system has been studied theoretically for a number of years, because when rolled up they form carbon nanotubes[2]. The material is unique because the underlying honeycomb lattice has a band structure with Dirac points at the corners of the Brillouin zone, two of which are inequivalent. Undoped, the system has one electron per atom and the Fermi energy surface passes directly through the Dirac points. For low energies and dopings the system may be described by the Dirac equation.

The stabilization of flat graphene sheets has allowed the application of perpendicular magnetic fields and the observation of the integer quantized Hall effect[3,4]. The striking result in these experiments is the first step height in the Hall conductance as a function filling factor, corresponding to filling the lowest Landau level (with electrons or holes), is *half* that of all subsequent steps. This behavior was expected[5] based on the bulk energy spectrum of graphene in a magnetic field: for a given spin species, there are pairs of Landau level bands at positive energies, each with partners at negative energies due to particle-hole symmetry. The lowest Landau level (LLL) has two levels precisely at zero energy, each of which is its own particle-hole conjugate[2]. This property of the LLL results in its smaller contribution to the Hall conductance.

The recent experiments on graphene studied ribbons that were relatively narrow, with widths in the micron[4] or submicron[3] range. Under such circumstances, transport in the quantum Hall regime is typically dominated by edge states[6]. In this work we study edge states for graphene ribbons in detail, focusing on the simplest cases of a zigzag edge and an armchair edge. We demonstrate that a continuum description of edge states based on the Dirac equation is possible with the adoption of appropriate boundary conditions. In an edge state description, the quantization of the Hall conductance is determined by the number of edge state bands crossing the Fermi level. The Hall conductance results imply that the LLL supports only a single particle-like and a single hole-like band (per spin) at each edge, while the higher Landau levels have twice as many. Our goal is to understand how and why this happens, in a non-interacting picture. (Because real spin plays no role in this study, we will from here on assume that all the electrons are spin-polarized, and refrain from explicitly noting the spin degree of freedom in our discussions.)

We now summarize our results. For zigzag edges, we show the correct boundary condition is for the wavefunction to vanish on a single sublattice across the edge. In this case the LLL supports two types of edge states, which we call current-carrying and dispersionless surface states. Both states have strong components at the boundary of the system, but the former has equal weights on both types of sites of the honeycomb lattice, whereas the latter exists essentially only on one sublattice and has precisely zero energy. Such zero energy surface states are well-known to exist in graphene ribbons in the absence of a magnetic field[7,8], and have been shown in tight-binding calculations to persist when a field is applied[9]. In the quantum Hall context we find that the dispersionless surface states play a special role in forming two branches of edge states that do not pass through the Fermi level for any non-zero doping. The current-carrying edge states are also remarkable in that the surface contribution on one sublattice can be highly separated from a component well-inside the bulk of the sample, on the other sublattice. An interesting consequence of this is that a particle injected near a zigzag edge should oscillate back and forth between the edge and bulk, although presumably such oscillations would be damped by many-body effects not included in our study.

For armchair edges, we find the correct boundary condition is vanishing of the wavefunction on both sublattices at the edge. This is achieved by mixing of wave-

functions from both Dirac points. In this case, there are no dispersionless surface states, and the LLL edge states behave differently than the higher Landau levels for other reasons. As we shall see, the energetics of states from one of these valleys is generically higher than from the other on a given sublattice, so that in the LLL only one band of edge states can meet the boundary condition, whereas in higher Landau levels there are two such bands. The admixing of the two valleys leads to wavefunctions with a characteristic spatial oscillation of the electron density with wavevector equal to ΔK_x, the difference between the Dirac point wavevectors along the direction perpendicular to the edge. Such oscillations should be observable in STM measurements.

II. PRELIMINARIES

We begin by reviewing some generalities about electrons in graphene. The lattice structure is a triangular lattice whose primitive lattice vectors are $\mathbf{a} = a_0(1,0)$ and $\mathbf{b} = a_0(1/2, \sqrt{3}/2)$. There are two atoms per unit cell located at $(0,0)$ and at $\mathbf{d} = a_0(0, 1/\sqrt{3})$. A simple tight-binding model with only nearest neighbor hopping t leads to a Hamiltonian with Dirac points at the six corners of the Brillouin zone, only two of which are inequivalent, and we take these to be $\mathbf{K} = \frac{2\pi}{a_0}(\frac{1}{3}, \frac{1}{\sqrt{3}})$ and $\mathbf{K}' = \frac{2\pi}{a_0}(-\frac{1}{3}, \frac{1}{\sqrt{3}})$. Wavefunctions can be expressed via the $\mathbf{k}\cdot\mathbf{P}$ approximation[2,10] in terms of envelope functions $[\psi_A(\mathbf{r}), \psi_B(\mathbf{r})]$ and $[\psi'_A(\mathbf{r}), \psi'_B(\mathbf{r})]$ for states near the $\mathbf{K}$ and $\mathbf{K}'$ points, respectively. These can be conveniently combined into a 4-vector $\Psi = (\psi_A, \psi_B, -\psi'_A, -\psi'_B)$. (The reason for this sign convention will become apparent when we discuss the armchair edge.) This satisfies a Dirac equation $H\Psi = \varepsilon\Psi$,

$$H = \gamma a_0 \begin{pmatrix} 0 & -k_x + ik_y & 0 & 0 \\ -k_x - ik_y & 0 & 0 & 0 \\ 0 & 0 & 0 & k_x + ik_y \\ 0 & 0 & k_x - ik_y & 0 \end{pmatrix}, \tag{1}$$

with $\gamma = \sqrt{3}t/2$. Note that $\mathbf{k}$ denotes the separation in reciprocal space of the wavefunction from the $\mathbf{K}$ ($\mathbf{K}'$) point in the upper left (lower right) block of the Hamiltonian. To apply this Hamiltonian in the presence of a magnetic field, one makes[2] the Peierls substitution $\mathbf{k} \to -i\nabla + e\mathbf{A}/c$ where $\mathbf{A}$ is the vector potential.

Before applying this procedure to systems with an edge, we point out some interesting and useful properties of H. Firstly, H (and the more exact tight-binding Hamiltonian from which it descended) has[8] chiral (i.e., particle-hole) symmetry, $\Gamma H \Gamma = -H$, where $\Gamma = \begin{pmatrix} \sigma_z & 0 \\ 0 & \sigma_z \end{pmatrix}$, and σ_z is the Pauli matrix. This tells us that a solution to the Dirac equation Ψ with energy ε has a particle-hole conjugate partner $\Gamma\Psi$ with energy $-\varepsilon$. Because of this, the wavefunctions must be normalized on each sublattice separately: $\int d\mathbf{r}[|\psi_\mu(\mathbf{r})|^2 + |\psi'_\mu(\mathbf{r})|^2] = 1/2$, for $\mu = A, B$. The solutions for states well away from the edge are well-known[2]. Taking $\mathbf{A} = -Bx\hat{y}$, $\Psi = \frac{1}{\sqrt{L_y}} e^{ik_y y}\Phi$, and $\psi_\mu(') = \frac{1}{\sqrt{L_y}} e^{ik_y y}\varphi_\mu(')$ with L_y the $\hat{y}$ extension of the sample, the wavefunctions retain their valley index as a good quantum number, and the positive energy wavefunctions may be written as $\Phi = [\phi_{n-1}(x-(k_y+K_y)\ell^2), \phi_n(x-(k_y+K_y)\ell^2), 0, 0]$ for the $\mathbf{K}$ valley, and $\Phi = [0, 0, \phi_n(x-(k_y+K'_y)\ell^2), -\phi_{n-1}(x-(k_y+K'_y)\ell^2)]$ for the $\mathbf{K}'$ valley, with energies $\varepsilon_n = \frac{\gamma a_0}{\ell}\sqrt{2n}$. In these expressions, ϕ_n is the nth harmonic oscillator state and $\ell = \sqrt{eB/c}$ is the magnetic length. The negative energy states are easily obtained by reversing the signs of the wavefunctions on the B sublattice. For the case of the LLL, $n = 0$, and only one component of the 4-vectors for each valley is non-zero. This means the particle-hole conjugate of these wavefunctions are themselves. The bulk LLL wavefunctions do not have a clear particle- or hole-like character.

III. ZIGZAG EDGE

The geometry for a zigzag edge is illustrated on the top and bottom edges of Fig. 1. It is interesting to note that each atom at the edge is of the same sublattice (say A). We shall see below that the appropriate boundary condition is to set the wavefunction to zero on a single sublattice (B), which we can understand to be the line of lattice sites that would lie just above or below the system if the bonds had not been cut to form the edge. In our discussions we will work with edges that lie along the $\hat{y}$ direction, so in what follows the coordinate axes in Fig. 1 will be rotated by 90°. We begin by computing the band structure for a tight binding model of a graphene ribbon with zigzag edges, an example of which is illustrated in Fig. 2. The flat degenerate bands over a range of k_y are Landau levels, and, in the case of the LLL, dispersionless surface states which we discuss below. In a wide sample, there is generically a large degeneracy within each Landau band, because for the $\mathbf{K}$ ($\mathbf{K}'$) valley there are wavefunctions peaked at $X_p = [k_y + K_y(') + nG_y]\ell^2$, where G_y is a reciprocal lattice vector for the ribbon, and the integer n can take any value such that X_p is between the sample edges. One may conveniently reorganize the states by allowing all values of k_y such that $-L_x/2 < [k_y + K_y(')]\ell^2 < L_x/2$, with L_x the ribbon width, and assigning one state for each k_y in the extended zone.

The prominent structure in Fig. 2 is the appearance of dispersing energy bands, which occur when the wavefunctions approach the edges. For the higher Landau levels one observes two pairs of such bands, whereas for the LLL there is only one such pair. This means that a Fermi energy crossing between the nth and $(n+1)$th Landau levels yields a Hall conductance $\sigma_{xy} = (2n+1)e^2/h$, as observed in experiment[3,4].

The unique behavior of the LLL edge states may be

understood in terms of eigenstates of the Dirac Hamiltonian with vanishing boundary conditions on a single sublattice. We begin by rotating the wavevectors in Eq. 1, $k_x \to k_y$, $k_y \to -k_x$ so that the zigzag edge lies along the $\hat{y}$, and our wavefunctions then exist in the space $x > 0$. Taking $\mathbf{A} = -Bx\hat{y}$ in this coordinate system, and defining the ladder operator $a = \frac{\ell}{\sqrt{2}}[-\tilde{k}_y + x/\ell^2 + \partial_x]$, with $\tilde{k}_y = k_y + K_y(')$ for the $\mathbf{K}$ ($\mathbf{K}'$) valley, the wavefunctions obey

$$\frac{2\gamma^2 a_0^2}{\ell^2} a a^\dagger \varphi_A = \varepsilon^2 \varphi_A, \quad \frac{2\gamma^2 a_0^2}{\ell^2} a^\dagger a \varphi_B = \varepsilon^2 \varphi_B \qquad (2)$$

$$\frac{2\gamma^2 a_0^2}{\ell^2} a^\dagger a \varphi'_A = \varepsilon^2 \varphi'_A, \quad \frac{2\gamma^2 a_0^2}{\ell^2} a a^\dagger \varphi'_B = \varepsilon^2 \varphi'_B. \qquad (3)$$

It is easy to see if one solves the equations for φ_B and φ'_A, the remaining wavefunctions are determined by $\varphi_A = a\varphi_B/\varepsilon$ and $\varphi'_B = -a\varphi'_A/\varepsilon$.

For the zigzag edge, the boundary condition does not admix valleys, and we can meet it for each type of wavefunction separately: $\varphi_B(x=0) = \varphi'_B(x=0) = 0$. Thus for the $\mathbf{K}$ valley the spectrum $\varepsilon_n^2(k_y)$ is identical to that of a quantum Hall edge with a sharp boundary[11]. The wavefunctions $\varphi_{B,n}$ similarly are identical to their standard Hall edge counterparts, turning into states in the nth Landau level as $k_y\ell^2$ moves well away from the edge. For $n \geq 1$, $\varphi_{A,n}$ is quite similar to a state in the $(n-1)$ Landau level provided the center of the wavefunction is not too close to the edge.

In the LLL ($n = 0$), φ_A is qualitatively different. Because LLL states are annihilated by the ladder operator a, and φ_B is similar to a bulk LLL state when the center of the wavefunction is not too close to the edge, φ_A is extremely small, except close to $x = 0$ where φ_B vanishes and is forced to deviate from a bulk LLL state. The result is that φ_A is strongly confined to the surface, and as the center of the φ_B moves further into the interior of the sample, φ_A becomes increasingly so confined. Despite this strongly localized form, the normalization of the wavefunctions discussed in the previous section requires that fully half the probability of finding the electron resides in this surface contribution. We note that, because ε disperses with k_y, these surface states carry current and contribute to the Hall conductivity.

Within the Dirac equation, the existence and form of these current-carrying surface states can be examined with a variational approach. We adopt a trial wavefunction $\varphi_B(x) = w(x)\phi_0(x - k_y\ell^2)$ and require $w(x \to 0) = 0$. One may easily confirm that $\tilde{\varepsilon}^2 = 2\int_0^\infty dx \left(\frac{dw}{dx}\right)^2 |\phi_0|^2$, where $\tilde{\varepsilon} = (\ell/\sqrt{2}\gamma a_0)\varepsilon$. A simple choice for w is $w = c_B(1 - e^{-\lambda x})$, where c_B is a normalization constant and our variational parameter is λ. With this choice one finds $\varphi_A(x) \propto \exp\{-[x - (k_y - \lambda)\ell^2]^2/2\ell^2\}$, so that if $\lambda > k_y$, φ_A is confined to the surface. The result of minimizing $\tilde{\varepsilon}^2$ is illustrated in Fig. 3, where in the inset one sees that λ increases faster than k_y, so that φ_A becomes more confined to the surface of the sample as k_y increases and φ_B penetrates into the bulk.

Direct examination of wavefunctions from the tight-binding model confirms this basic picture, except in one important respect. Whereas the Dirac equation allows current carrying states with φ_A increasingly localized to the surface as k_y grows (and the peak position X_p of φ_B moves into the bulk), the tight-binding results show that for $X_p > \frac{1}{2}|K_y - K'_y|\ell^2$ the LLL wavefunction on sublattice A and the surface state on sublattice B appear as separate states, and that the surface state now moves back into the interior of the system with further increase in k_y. The current-carrying surface state evolves into a dispersionless surface state which we describe below, and the number of allowed current-carrying surface states is limited. This is clearly an effect of the discreteness of the lattice that is not captured by the Dirac equation: independent, highly localized surface states can be written down for any k_y in the continuum, but on the lattice states at k_y and $k_y + G_y$ have the same periodicity along the $\hat{y}$ direction, and so cannot be made independent. Thus the number of current-carrying surface states is limited to $\sim L_y|K_y - K'_y|/4\pi$. For any practical purpose, this may be imposed by introducing a cutoff k_c in the allowed k_y's for the current-carrying surface states. For $k_y > k_c$, one may take the $\mathbf{K}$ valley wavefunction to have its bulk form.

The edge state wavefunctions of the $\mathbf{K}'$ valley on the A sublattice are analogously identical to the well-known ones[11], although ε_n^2 is shifted upward by a single unit ($2\gamma^2 a_0^2/\ell^2$) due to the ordering of the operators in the last of Eqs. 3. For the LLL, the bulk states $\varphi'_A \propto \phi_0(x - X'_p)$, $\varphi'_B = 0$, with $X'_p = k_y\ell^2 - K'_y\ell^2$, exactly satisfy Eqs. 3 with zero energy. Remarkably, these states are unaffected by the edge. Moreover, because $K'_y \neq K_y$, there are values values of k_y in the extended zone for which $X'_p < 0$, and the state is confined to the surface. These are the dispersionless surface states: they do not contribute to the Hall conductivity. The LLL wavefunctions of the tight-binding results around the center of the bands in Fig. 2(a) behave precisely as the Dirac equation results suggest: they are strongly confined to the surface, and continuously evolve into bulk LLL states on the A sublattice as k_y increases. The dispersionless surface states supported by the LLL are the reason that it carries only half the Hall conductivity of the higher Landau levels for the zigzag edge[12].

IV. ARMCHAIR EDGE

The armchair edge is illustrated as the left and right edges Fig. 1, and the corresponding bandstructure from a representative tight-binding calculation appears in Fig 2(b). Here the edge runs along the $\hat{y}$ direction, and no rotation of the figure is needed to represent our calculations. Unlike the zigzag edge, the Landau bands all have dispersing states in the same regions of k_y, but the LLL has one pair each of hole-like and particle-like edge states, while all the higher Landau levels have two.

To understand this from the viewpoint of the Dirac equation, we need to impose appropriate boundary conditions. In Fig. 1 one may see that the termination consists of a line of A-B dimers, so it is natural to have the wavefunction amplitude vanish on both sublattices at $x = 0$. To do this we must admix valleys, and require $\varphi_B(x = 0) = \varphi'_B(x = 0)$ and $\varphi_A(x = 0) = \varphi'_A(x = 0)$. Using the Dirac equation, and the fact that $K_y = K'_y$, this second condition implies $\partial_x\varphi_B|_{x=0} = -\partial_x\varphi'_B|_{x=0}$. To understand the effect of this on the solutions, it is convenient to combine the φ_B's into a single wavefunction defined for $-\infty < x < \infty$: $\psi(x) = \varphi_B(x)\theta(x) + \varphi'_B(-x)\theta(-x)$, with $\theta(x)$ the step function. The boundary conditions then amount to $\psi(x)$ and its derivative being continuous at $x = 0$. (This was the reason for our choice of relative sign in the 4-vectors of Section II.) From Eqs. 2 and 3, it is easy to see that ψ obeys a Schroedinger equation $[-\partial_x^2 + U(x)]\psi(x) = \tilde{\varepsilon}^2\psi(x)$, with $U(x) = \frac{\ell^2}{2}\left[(|x|/\ell^2 - k_y)^2 - 1/\ell^2 + (2/\ell^2)\theta(-x)\right]$. For large $k_y\ell^2$, this double well potential, illustrated in Fig. 4, has low energy states associated with the left well at $\tilde{\varepsilon}^2 \approx 3/2,\ 5/2, \ldots$, while for the right well one has states at $\tilde{\varepsilon}^2 \approx 1/2,\ 3/2,\ 5/2, \ldots$. We thus see there will be hybridization leading to pairs of edge states for all the higher Landau levels, whereas for the LLL there will be just a single such state.

The admixing of different valley states to meet the boundary condition means that the wavefunction will oscillate with period $2\pi/|K_x - K'_x|$. The behavior can explicitly be seen in Fig. 5, which illustrates a LLL edge state from the tight-binding calculation. The apparent oscillation has precisely the period one expects for the valley mixing we introduced in the Dirac equation to meet the boundary condition. Although the period of this oscillation is very short (3.69Å), it is in principle observable by STM measurements because the samples can be open to their environment[3], in contrast to GaAs systems.

V. CONCLUSION

In this paper we have studied the edge states of graphene ribbons with zigzag and armchair terminations. We found in both these cases that a continuum description in the form of the Dirac equation captures most features of the states found in tight-binding calculations, provided the wavefunction vanishes at the termination of the sample. For zigzag edges, we found the boundary condition can be met by wavefunctions within a single valley, leading to two types of edge states in the lowest Landau level, current-carrying surface states and dispersionless surface states. The latter of these explains why the contribution to the quantized Hall coefficient from the LLL is only half that of higher Landau levels. For the armchair edge, we found that admixing of valleys is necessary to satisfy the boundary condition. For higher Landau levels, there are two hybridizations of the valley states for which this is possible, whereas in the LLL there is only one. This again leads to a contribution to the Hall coefficient from the LLL half the size of those from other occupied Landau levels.

Acknowledgements. The authors thank F. Guinea and C. Tejedor for useful discussions. This work was supported by MAT2005-07369-C03-03 (Spain) (LB) and by the NSF through Grant No. DMR-0454699 (HAF).

[1] K.S. Novoselov et al., Science **306**, 666 (2004).
[2] For a recent reviews, See T. Ando, J. Phys. Soc. Jpn. **74**, 777 (2005) and F. Guinea, M. López-Sancho, and M. Vozmediano, cond-mat/0511558 (2005), and references therein.
[3] K.S. Novoselov et al., Nature **438**, 197 (2005).
[4] Y. Zhang et al., Nature **438**, 201 (2005).
[5] Y. Zheng and T. Ando, Phys. Rev. B **65**, 245420 (2002); V.P. Gusynin and S.G. Shaparov, Phys. Rev. Lett. **95**, 146801 (2005).
[6] For a review, see article by C.L. Kane and M.P.A. Fisher in *Perspectives in Quantum Hall Effects*, S. Das Sarma and A. Pinczuk, Eds. (Wiley, New York, 1997).
[7] K. Nakada, M. Fujita, F. Dresselhaus, and M. Dresselhaus, Phys. Rev. B **54**, 17954 (1996);.
[8] S. Ryu and Y. Hatsugai, Phys. Rev. Lett. **89**, 077002 (2002).
[9] A.H. Castro-Neto, F. Guinea, and N.M.R. Peres, cond-mat/0509709 (2005).
[10] D.P. DiVincenzo and E.J. Mele, Phys. Rev. B **29**, 1685 (1984).
[11] B.I. Halperin, Phys. Rev. B **25**, 2185 (1982).
[12] Terms that break the particle-hole symmetry (e.g., next nearest neighbor hopping) can introduce an energy dependence in the dispersionless surface states. However, the resulting edge states are not chiral and do not contribute to the Hall conductivity. See Ref. 9.

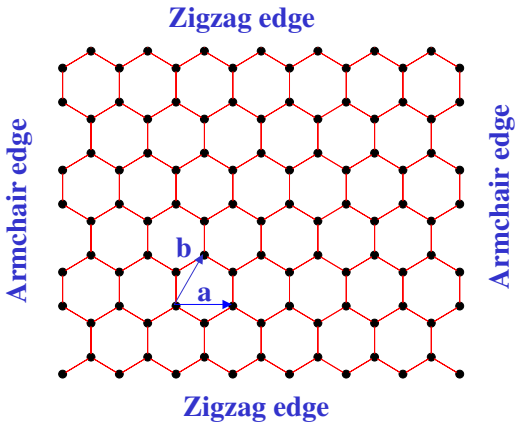

FIG. 1: Ilustration of a graphene system with edges. Top and bottom edges are zigzag edges, left and right are armchair edges.

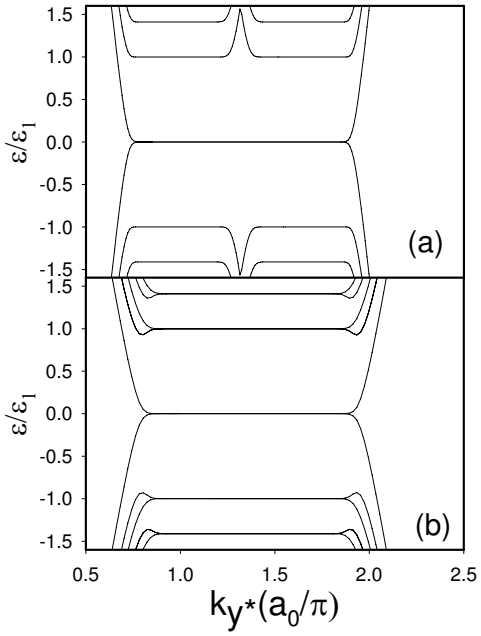

FIG. 2: Examples of energy bands for a graphene ribbon with periodic boundary conditions in the $\hat{y}$ direction and edges in the $\hat{x}$ direction. B=100T (0.00126 flux quanta per unit cell.) Unit of energy $\varepsilon_1 = \sqrt{2}\gamma a_0/\ell$. (a) Ribbon with zigzag edges, 500 sites (530Å) wide. (b) Ribbon with armchair edges, 1000 sites (460Å) wide.

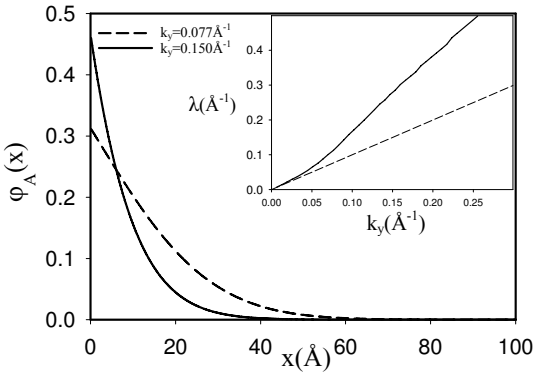

FIG. 3: Surface part of current-carrying edge state for zigzag edge from variational method described in text. Main figure: φ_A for two different choices of k_y. Inset: λ_{min} (solid line) vs. k_y (dashed line), demonstrating that φ_A becomes increasingly localized on the surface with increasing k_y.

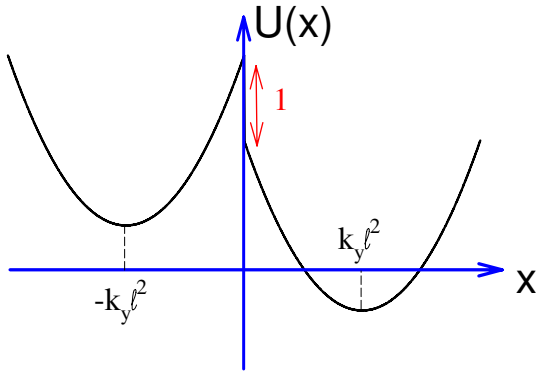

FIG. 4: Potential $U(x)$ for an armchair edge. See text.

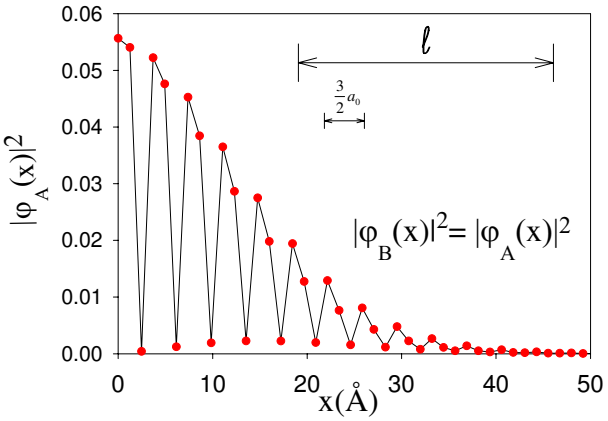

FIG. 5: Squared wavefunction for an edge state of the armchair edge from tight binding calculation. $k_y = 2.1\pi/a_0$ and $\varepsilon/\varepsilon_1 = -0.202$. Wavefunction penetrates sample over length scale ℓ, while oscillations due to valley mixing occur on a much smaller length scale $(3a_0/2)$.